Title	Fault Detection in Distribution Networks in Presence of Distributed Generations Using a Data Mining Driven Wavelet Transform
Authors(s)	Mohammadnian, Youness; Amraee, Turaj; Soroudi, Alireza
Publication date	2018-12-26
Publication information	IET Smart Grid, eFirst : 1-9
Publisher	IET
Item record/more information	http://hdl.handle.net/10197/9740
Publisher's statement	This is an open access article published by the IET under the Creative Commons Attribution-NoDerivs License (http://creativecommons.org/licenses/by-nd/3.0/)
Publisher's version (DOI)	10.1049/iet-stg.2018.0158

Fault Detection in Distribution Networks in Presence of Distributed Generations Using a Data Mining Driven Wavelet Transform

Youness Mohammadnian[1], Turaj Amraee[1]*, and Alireza Soroudi[2]

[1] Faculty of Electrical Engineering, K. N. Toosi University of Technology, Tehran, Iran.

[2] University College Dublin, Dublin, Ireland.

* *amraee@kntu.ac.ir*

Abstract—In this paper, a data mining driven scheme based on discrete wavelet transform (DWT) is proposed for high impedance fault (HIF) detection in active distribution networks. Correlation between the phase current signal and the related details of the current wavelet transform is presented as a new index for HIF detection. The proposed HIF detection method is implemented in two subsequent stages. In the first stage, the most important features for HIF detection are extracted using support vector machine (SVM) and decision tree (DT). The parameters of SVM are optimized using the genetic algorithm (GA) over the input scenarios. In second stage SVM is utilized to classify the input data. The efficiency of the utilized SVM based classifier is compared with a probabilistic neural network (PNN). A comprehensive list of scenarios including load switching, inrush current, solid short circuit faults, HIF faults in the presence of harmonic loads is generated. The performance of the proposed algorithm is investigated for two active distribution networks including IEEE 13-Bus and IEEE 34_Bus systems.

Keywords-- High impedance fault, active distribution network, discrete wavelet transform, correlation, data mining

1. Introduction

High impedance faults could not be detected by insensitive overcurrent protective relays due to low fault current in distribution networks. High impedance faults often occur when the conductor is broken and comes into contact with high impedance surfaces such as branches of a tree. Because of low fault current the main objective of HIF detection is not to protect the system, but to protect the human and animals lives and prevent fire hazards [1].

The HIF detection methods are categorized into time domain methods, frequency domain techniques, time-frequency domain methods and intelligent methods. Current or voltage waveforms of HIF faults have some unique characteristics due to nonlinearity and randomness of these faults. Proportional relaying [2], ratio ground relaying [3], fault current flicker and half-cycle asymmetry [4] and fractal techniques [5] are examples of time domain methods for HIF detection. Because of the arcing phenomenon during this fault, current waveform of HIF contains low and high-frequency components. Frequency domain algorithms use third harmonics [6], second-fourth-sixth harmonics [7] and high-frequency components (2-10 kHz) of fault current to detect HIF faults [8]. Another category of HIF detection methods is the time-frequency domain technique, in which some features of high impedance fault is detected based on discrete wavelet transform [9-12], S transforms [13-14] and Kalman filtering [15]. Intelligent methods act based on training over a given predetermined scenario such as decision tree [16], neural networks [1],[17-18], ANFIS algorithms [19] and support vectors machine [13], [20-22].

Some recent works have proposed new method for HIF detection. The proposed method In [23] detects HIF faults using the even harmonics of the voltage waveforms measured by smart meters. In [24] the proposed algorithm utilizes mathematical morphology (MM) techniques for HID detection based on filtering functions. In [25] the authors utilize one-cycle sum of superimposed components of residual voltage the maximum value of one-cycle sum of superimposed components of negative-sequence current for HIF detection. In [26] a transient-based algorithm for HIF detection in distribution systems has been developed using the discrete wavelet transform.

To increase reliability and security of HIF detection method, it's necessary to present more effective features with high information gain. For this purpose in this paper, a two-stage scheme is presented using DWT. In the first stage, the feature selection is carried out using SVM technique. Based on DWT, the correlation between phase current signal and its details is presented as a new HIF predictor. In the second stage, some classifier methods are utilized to detect HIF conditions. The performance of the proposed index is compared through a general proposed structure to other classification methods via the dependability and security criterion. The two major advantages of the current work with respect to the method discussed in literature review are: a) The correlation between phase current signal and its details is presented as a new HIF predictor. This feature needs just the current signal, and b) Optimizing the SVM parameters using GA algorithm.

This paper is organized as follows. In section 2, the general structure of proposed method is explained. Section 3 describes the simulation results of the proposed algorithm based on the security and dependability criterion. Finally, the conclusion is given in section V.
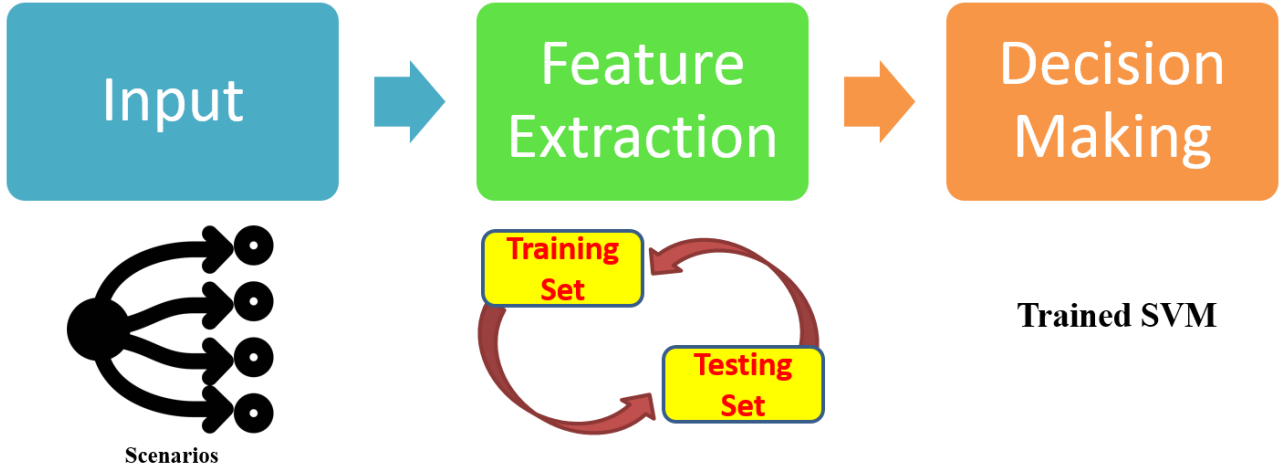
Fig. 1. The proposed HIF detection method

2. HIF detection scheme

Generally data mining techniques for HIF detection have two major parts. In the first part, a classifier is trained using a large number of input-output training scenarios. These scenarios include all credible HIF and non-HIF conditions. In other word, the first part is an offline procedure to construct the HIF classifier. The second part is devoted to the application of trained classifier for the online detection of HIF fault. Indeed, the second part has a very low computational burden and could identify the HIF in a fraction of second.

The flowchart of the proposed HIF detection method is depicted in Fig.1 Based on this structure the proposed method has three major parts including generating input scenarios, feature extraction, and HIF detection. Each part is described as follows:

A. Feature extraction

In this paper, feature extraction is carried out by wavelet transform. The most important features are extracted using discrete wavelet transform. DWT is utilized to determine the approximation and details coefficients of fault current signal. The correlation of fault current signal with its details is developed as a HIF detection feature.

1) Discrete wavelet transform

DWT can provide time and frequency domain characteristics simultaneously. In DWT, the scaling function is given by (1), and wavelet function as given in (2) is used to decompose the signal to different levels.

$$\emptyset_{j,k}(t) = 2^{j/2}\emptyset(2^j t - k) \quad , \quad -\infty < j, k < +\infty \quad (1)$$

$$\varphi_{j,k}(t) = 2^{j/2}\varphi(2^j t - k) \quad -\infty < j, k < +\infty \quad (2)$$

According to [27], $\emptyset(t)$ and $\varphi(t)$ can be expressed in terms of a weighted sum of shifted $\emptyset(2t)$ and $\varphi(2t)$ as:

$$\emptyset(t) = \sum_n h(n)\sqrt{2}\emptyset(2t - n) \quad n \in Z \quad (3)$$

$$\varphi(t) = \sum_n g(n)\sqrt{2}\varphi(2t - n) \quad n \in Z \quad (4)$$

where $h(n)$ are scaling function coefficients and $g(n)$ can be obtained by (5).

$$g = (-1)^n h(1 - n) \quad (5)$$

After the first level of decomposition, DWT divides input signals into high frequency and low-frequency sub-bands by high pass and low pass filters. Therefore the input signal can be rebuilt using its approximation and detail coefficients as given by (6).

$$x(t) = \sum_{k=-\infty}^{+\infty} a_{j_m}(k)\emptyset_{j-j_m,k}(t)$$
$$+ \sum_{k=-\infty}^{+\infty} \sum_{L=1}^{j_m} d_L(k)\varphi_{j-L,k}(t) \quad (6)$$

where

$$a_j = \langle x(t), \emptyset_{j-1,k}(t) \rangle$$
$$= \int x(t) \, 2^{(j-1)/2}\emptyset(2^{(j-1)}t - k) \quad (7)$$

By using (3) and (7), (8) can be written as

$$\emptyset(2^{j-1}t - k) = \sum_n h(n)\sqrt{2}\emptyset(2(2^{j-1}t - k) - n) \quad (8)$$

By assuming that $m = 2k + n$, (8) and (7) are written as follows.

$$\emptyset(2^{j-1}t - k) = \sum_n h\,(m - 2k)\sqrt{2}\emptyset(2^j t - m) \qquad (9)$$

$$a_j = \sum_m h\,(m - 2k)\int x(t)\,2^{j/2}\,\emptyset(2^j t - m)dt \qquad (10)$$

Finally, the approximations and details of the input signals are determined as given by (11) and (12) respectively.

$$a_j(k) = \sum_m h\,(m - 2k)a_{j-1}(m) \qquad (11)$$

$$d_j(k) = \sum_m g\,(m - 2k)a_{j-1}(m) \qquad (12)$$

After the first level of signal decomposition, a high pass and low pass signals are obtained. This process is then applied on low pass signal for several levels. Fig.2 shows signal decomposition using high and low pass filters into three levels. The output of low pass decomposition (i.e. a_j) and high pass decomposition (i.e. d_j) give the approximation and detail coefficients respectively.
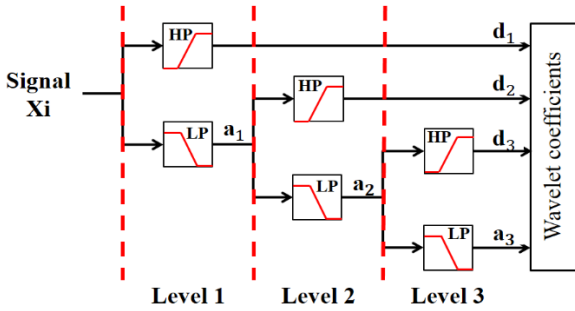

Fig. 2. Decomposing signal using DWT

2) Correlation coefficient

Covariance is an index that shows the dependence between two variables. For two vectors X and Y the Covariance will be defined as (13).

$$COV(X,Y) = \frac{1}{n}\sum_{i=1}^{n}(X_i - \mu_X)(Y_i - \mu_Y) \qquad (13)$$

where μ_x and μ_y are means of X and Y respectively. If there is no correlation between two vectors, their covariance will be equal to zero and they have no linear dependency. The amount of correlation coefficient for continuous and discrete variables is calculated using (14) and (15) respectively.

$$Correlation(X,Y) = \frac{COV(X,Y)}{\sqrt{Var(X).Var(Y)}} \qquad (14)$$

$$Correlation(X,Y)$$
$$= \frac{\sum_{i=1}^{n}(X_i - \mu_X)(Y_i - \mu_Y)}{\sum_{i=1}^{n}(X_i - \mu_X)\sum_{i=1}^{n}(Y_i - \mu_Y)} \qquad (15)$$

The value of correlation coefficient given by (14) varies between -1 and +1. The correlation of detail coefficients of phase current signal in DWT is developed as a new feature for HIF detection. For calculating the new index, phase current signal, and related detail coefficients are needed Correlation coefficient between these two signals as a new feature is explained in (16).

$$Correlation(X, d_k)$$
$$= \frac{\sum_{i=1}^{n}(X_i - \mu_X)(d_{k,i} - \mu_{d_{k,i}})}{\sum_{i=1}^{n}(X_i - \mu_X)\sum_{i=1}^{n}(d_{k,i} - \mu_{d_{k,i}})}, k = 1,2,\dots,8 \qquad (16)$$

This feature can provide remarkable information gain for distinguishing high impedance faults. DWT is applied to all simulated scenarios, and the extracted details are recorded as vectors. The value of correlation between every detail coefficients of the wavelet transform in each level and phase current signal is computed using (16). The developed correlation coefficients along with the other indices are used as input features for HIF detection.

B. Dimension reduction methods

A critical goal in pattern recognition problem or data classification is finding the optimal combination of indices that classify data with high accuracy. The existence of redundant features besides the essential features will cause computational burden and complexity in classification systems. Therefore the classification systems may result in misclassification. By dimension reduction and feature selection, the computational burden of classification algorithm will be reduced, and extracted patterns can be easily implemented in hardware [28]. To reach this goal, the accuracy error in classification algorithm is considered as the fitness function in optimizing algorithm. The dataset is divided into training and test data. The error of classification for each subset will be examined by K-Fold cross-validation. The subset with minimum classification error will be chosen as the best subset of final features. In this paper, support vector machine is utilized to extract the optimal input features. The error of support vector machine is used as fitness function of genetic algorithm, and the best subset is then selected.

1) Support vector machine

Due to the nonlinearity of HIF phenomena, the nonlinear SVM algorithm is developed for HIF detection. The nonlinear SVM has two stages. In the first stage, input data is mapped to a higher dimension space. After that, in the second stage, the algorithm searches for linear separating hyperplanes in new space. The task of this stage is formulated as a quadratic optimization problem. In support vector machine the original finite-dimensional space may not be linearly separable. Therefore the original finite-dimensional space is mapped into a high-dimensional feature space. However, working with such high dimensional space increases the computational burden of classification. Therefore kernel functions are utilized. The kernel function is applied on initial data, and the dimension of these new data is lower than the initial data. Thus by using the kernel function the direct calculation of mapping function could be ignored [29].

$$Min \; \frac{1}{2}\sum_i \sum_j \alpha_i\,\alpha_j Y_i\,Y_j F(X_i)^T F(X_j)$$

$$= \frac{1}{2}\sum_i \sum_j \alpha_i\,\alpha_j Y_i\,Y_j K(X_i,X_j) \tag{17}$$

where

$$K(X_i,X_j) = F(X_i)^T F(X_j) \tag{18}$$

In this paper radial basis function (RBF) is utilized as the kernel.

$$K(X_i,X_j) = exp(-\frac{1}{2\delta^2}||X_j - X_i||^2) \tag{19}$$

where δ is the spread parameter of the kernel function. The objective function is formed for a specified number of inputs and the support vectors (SV) α_i are extracted by solving (9). For example the minimization of n input data like (X,Y) is performed as follows:

$$Min \; \frac{1}{2}\,\alpha^T H\alpha + f^T \alpha \tag{20}$$

s.t:

$$H = \sum_i \sum_j Y_i Y_j K(X_i,X_j)$$
$$f = -[1]_{n\times 1}$$
$$Y,\alpha = 0 \qquad 0 \le \alpha \le C$$

SV set includes Support Vectors which is expressed as given in (10):

$$Support\ Vectors: SV: \{i|\ 0 \le \alpha_i \le C\} \quad i = 1,2,\dots,n \tag{21}$$

In the next stage, the value of b can be obtained using SV as given in (22).

$$b = \frac{1}{|S|}\sum_{i\in S}(Y_i - \sum_j \alpha_i\,\alpha_j K(X_i,X)) \tag{22}$$

Finally the class label of test data is predicted as follows.

$$Outputs: \quad Y = Sign\,(\sum_j \alpha_i Y_i K(X_i,X) + b) \tag{23}$$

2) Dimension reduction

The genetic algorithm [30] is used for selecting the best features and determine the optimal parameters of SVM. In this paper, the classification error and the number of features are integrated to design the fitness function of GA algorithm. Therefore the fitness function value is minimum for any member of population which has the high accuracy and fewer features. The utilized fitness function is expressed as follows:

$$Fitness = W_A \times (1 - SVM_{accuracy})$$
$$+ W_F \times (\sum_{i=1}^{n_i} F_i) \tag{24}$$

where $SVM_{accuracy}$ is the accuracy of classification based on 5-fold cross-validation and n_i is the number of features. If features i is selected the value of F_i is equal to 1 and vice versa. W_A and W_F are weighting factors for error of classification and number of features. In this paper, the values of $W_A\ and\ W_F$ are assumed as 18 and 0.55 respectively.

Indeed a high priority is considered for the classification accuracy. Based on the required levels of accuracy and the maximum desired number of input features, these weighting factors can be adjusted properly. Without considering the second term of the fitness function (i.e. $W_F = 0$) the proposed classifier tends to select a high number of input features which is not practically preferred. Using these weighting factors, the proposed algorithm seeks for the minimum accuracy with minimum possible number of input features. It is noted that the premature convergence is a common problem in genetic algorithms, as it leads to a suboptimal solution due to rapid convergence. However there are some strategies to prevent this phenomenon such as increasing the population size or utilizing a uniform crossover.

3. Simulation results and discussion

In this section, the performance of the proposed method is verified. The proposed algorithm is implemented in IEEE 34-Bus and IEEE 13-Bus. The results of simulations are presented in six parts including modeling of test systems, HIF model, scenario generation, features extraction, dimension reduction and classification.

In this paper, db4 as a most common used mother wavelet in Daubechies family wavelets has been selected. This type of mother wavelet is asymmetric, orthogonal, and biorthogonal. The details of utilized mother wavelet are similar to the settings utilized in [10]. The sampling frequency is 10kHz. The scale of frequency conversion (i.e. the frequency bound) are assumed as (2.5kHz-5kHz), (1.25kHz-2.55kHz), (0.626kHz-1.25kHz), (0.313kHz-0.626kHz), and (0.157kHz-0.313kHz), for level 1 to level 5 of decomposition respectively.

A. Test systems

HIF and other similar events are simulated in Matlab/Simulink. Different scenarios are discussed in test systems with and without photovoltaic. Single line diagram IEEE 34-Bus and IEEE 13-Bus test systems are shown in Fig. 3. Data of IEEE 13-Bus test system and IEEE 34-Bus test grid could be found in [31]. It has been assumed that a photovoltaic generating unit is installed at bus 680 and bus 840 in IEEE 13-bus and IEEE 34-Bus test systems respectively. Data of this generating unit has been given in Table 1. Also the parameters of genetic algorithm have been reported in Table 2.
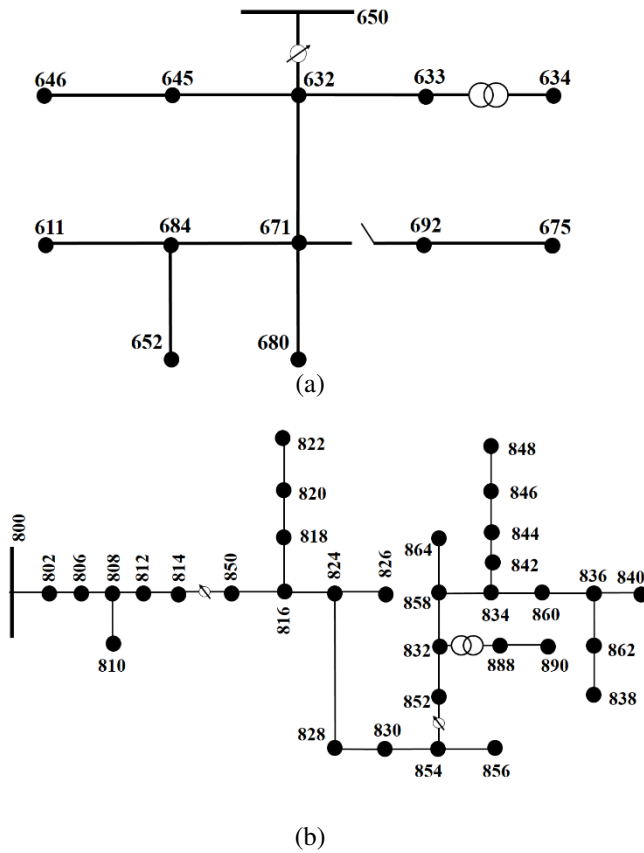
(a)

(b)

Fig. 3. Single line diagrams of the networks a) IEEE-13 Bus , b) IEEE-34 Bus

TABLE 1
PARAMETERS OF PV DISTRIBUTED GENERATOR

Parameter	Value
Inverter nominal 3-phase power	250 kVA
Nominal inverter primary line-to-line voltage	4.160kV
Nominal DC link voltage (V)	480 V
Nominal inverter secondary line-to-line voltage	250 V
Transformer nominal power	250 kVA
Transformer Leakage inductance	0.06 pu

TABLE 2
PARAMETERS OF GENETIC ALGORITHM

Parameter	IEEE 13-Bus	IEEE 34-Bus
Maximum Iteration	300	400
Number of Population	100	100
Percent of Crossover	0.80	0.80
Percent of Mutation	0.3	0.30

B. Model of HIF

This paper uses the modified Emanuel model for HIF which has been obtained based on actual tests [32].The HIF current in the steady state has half-cycle asymmetry and non-linear variations. According to Fig. 4 two resistances, R_p and R_n represent the fault resistance with different values that build asymmetric behavior of fault currents.
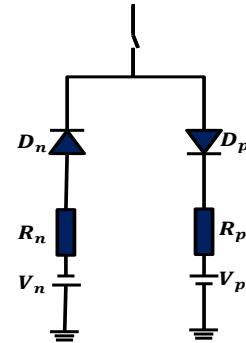

Fig. 4. Modified Emanuel arc model

In order to model the type of contact surfaces of HIF model two antiparallel DC sources are used. The amplitudes of these sources depend on the density and moisture of the soil. By decreasing the soil density and moisture the value of these DC sources are increased.

When a broken conductor falls on a high impedance surface, some arcs coincide. To model such nonlinearity this paper uses several HIF models in parallel as illustrated in Fig. 5. The fulfillment of the utilized HIF model is investigated by measuring some current harmonics such as third, fifth and seventh.

The current waveform for a given HIF condition has been depicted in Fig. 6. It has all steady state (i.e. asymmetric and nonlinear behavior) and transient (i.e. buildup and shoulder) characteristics.

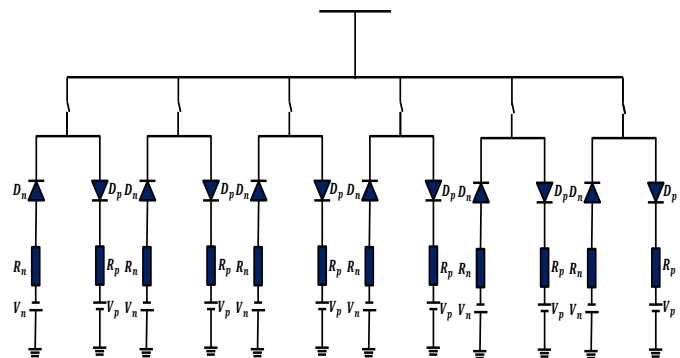According to Fig.7, the modified Emanuel HIF model produces characteristics similar to the actual HIF current.

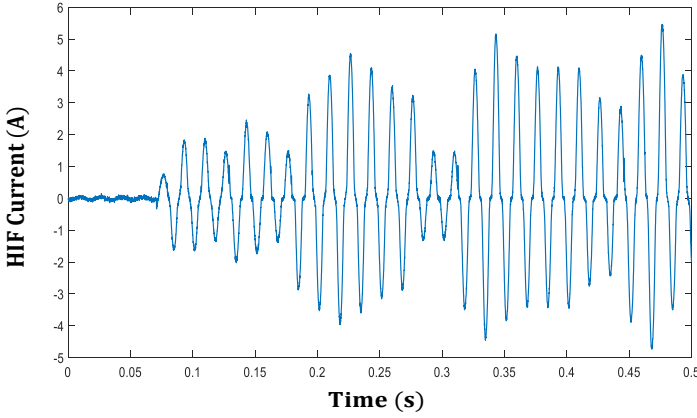
Fig. 5. Implemented model for HIF model

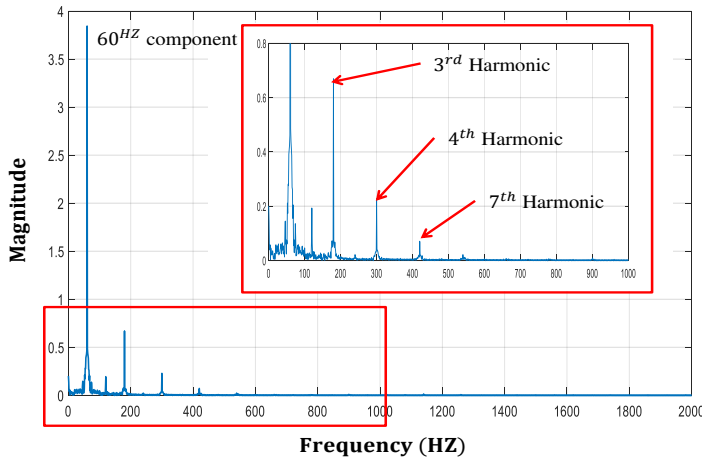Fig. 6. Fault current using modified Emanuel HIF model

Fig. 7. Frequency components of simulated HIF current

C. Simulated scenarios

To evaluate the proposed method, a comprehensive list of input scenarios including load switching, capacitor bank switching, transformer inrush current, nonlinear and harmonic loads and different short circuit faults are simulated. Also, different HIFs are simulated in variant states.

Table 3 describes the type of events and number of input scenarios. The total number of non-HIF and HIF scenarios in each of IEEE 13-Bus and IEEE 34-Bus are 494 and 582 scenarios respectively.

In this paper using DWT, the fault current signal at the substation is decomposed up to 8 levels. For each level of decomposition, the proposed correlation coefficient and some of the previously proposed features including energy, power, standard deviation, RMS, mean and entropy are then computed for all input scenarios. Eventually, the prepared data set includes 56 features.

The data set is randomly divided into the test and training parts (80 percent for training part and 20 percent for test part).

TABLE 3
DESCRIPTION OF SIMULATED EVENTS

Event Type	Number of Scenarios	
	IEEE 13-Bus	IEEE 34-Bus
Harmonic Loads	40	40
Load Switching	44	52
Inrush Current	42	42
Short circuit	192	192
Capacitor Switching	32	48
High Impedance Faults	144	208
Total	494	582

The performance of the proposed two-stage HIF detection is investigated over the input data. In the first stage, the feature selection (i.e. dimension reduction) is carried out using the optimized support vector machine. Using the extracted features, the HIF classification is then done using support vector machine. The performance of the classification method is compared with other methods based on security and dependability as follows [21]:

$$Dependebility = 100 \times \frac{number\ of\ HIFs\ detected\ as\ HIF}{number\ of\ all\ HIF\ cases}$$

$$Security = 100 \times \frac{number\ of\ NonHIFs\ detected\ as\ NonHIF}{number\ of\ all\ NonHIF\ cases}$$

D. Dimension reduction

In section II, the procedure of dimension reduction using GA and SVM algorithms was presented. The dimension of each sample in prepared data set for HIF detection is 56. It is noted that just some effective and important features are selected by using SVM and GA. Results of the proposed method are compared with DT feature selection results [33, 34]. Table 4 introduces the input features. The results of two methods imply that correlation index is one of the most important features.

TABLE 4
INPUT FEATURES DESCRIPTION FOR EIGHT DECOMPOSITION

Selected Feature	Description
$F_1, \dots, F_8$	Energy for detail coefficients
$F_9, \dots, F_{16}$	Power of Detail Coefficients
$F_{17}, \dots, F_{24}$	STD for Detail Coefficients
$F_{25}, \dots, F_{32}$	RMS for Detail Coefficients
$F_{33}, \dots, F_{40}$	Mean for Detail Coefficients
$F_{41}, \dots, F_{48}$	Entropy for Detail Coefficients
$F_{49}, \dots, F_{56}$	Correlation between phase current and details

E. Classification

In this section, the selected features are used as input features for HIF classification. The performance of classification methods is verified using the proposed indices. Tables 4 and 5 give the results of classification for both test system using the input features determined by the GA and DT algorithms respectively. Values of security and

dependability indices and accuracy of classification algorithm are reported in Tables 5 and 6. According to the obtained results it can be seen that the proposed correlation coefficient has increased the accuracy of the classification significantly. For IEEE 13-Bus system the features including F_{56}, F_{53}, F_{11} and F_8 are selected. Also, for IEEE 34-Bus system the features F_{53}, F_{49}, F_{24} and F_{17} are selected. In both selected subsets of features, the presented feature (correlation coefficients) is an efficient feature.

According to Table 4, the initial number of input features is equal to 56. According to Table 5, by the proposed weighting factors, the best accuracy is obtained just using 4 input features. Table 6 gives the information subsets of selected features by DT for both test systems. To reduce obtained by DT includes too many features, just the 6 features that have the highest information gain values would be selected as the selected features for classifying algorithms input.   In order to prove the efficacy of the correlation index, the classification accuracy, security and dependability indices without considering the correlation index has been reported in Table 6. It can be seen that without considering the correlation index the overall classification is reduced significantly. Comparison between Table 6 and Table 7 implies that the dimensions of selected features are increased by eliminating the correlation index. This issue incurs more computational burden and complexity in extracted patterns and hence the classifier efficacy is deteriorated accordingly.

TABLE 5
RESULTS FOR DIFFERENT HIF DETECTION METHODS USING SELECTED FEATURES BY GA

Method	dependability	Security	Train Accuracy	Test Accuracy
IEEE 13-Bus				
SVM	98.50	100	99.49	98.99
PNN	100	96.87	98.99	98.99
Feature	$F_{56} - F_{53} - F_{11} - F_8$			
IEEE 34-Bus				
SVM	97.14	100	100	98.27
PNN	97.14	100	100	98.27
Feature	$F_{53} - F_{49} - F_{24} - F_{17}$			
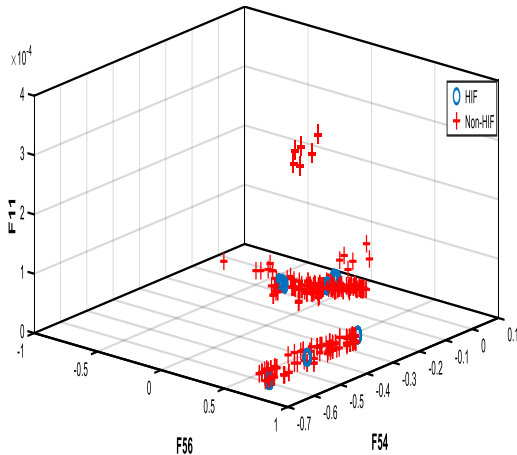
TABLE 6
RESULTS FOR DIFFERENT HIF DETECTION METHODS USING SELECTED FEATURES BY DT

| Method	dependability	Security	Train Accuracy	Test Accuracy
IEEE 13-Bus				
SVM	98.50	81.25	99.24	92.93
PNN	95.45	90.625	96.71	93.88
Feature	$F_{24} - F_{56} - F_{34} - F_{51} - F_3 - F_{55} - F_7 - F_1$			
IEEE 34-Bus				
SVM	97.14	97.83	99.14	97.41
PNN	91.43	100	99.14	94.83
Feature	$F_{20} - F_{44} - F_2 - F_{54} - F_{41} - F_{45}$			

In other words the proposed correlation index between the original fault current signal and its details will promote the overall accuracy of the HIF detection. Fig. 8, shows the best three-dimensional view of the three selected features obtained by GA-SVM in both simulated test cases.
Fig. 9 to Fig. 10 display the performance of the proposed method for a given HIF fault and a load switching event, respectively. In order to verify the effect of each event on detail coefficients, the noise is removed from the waveform of fault current signal.

TABLE 7
RESULTS OF HIF DETECTION METHODS USING SELECTED FEATURES BY GA WITHOUT CORRELATION INDEX

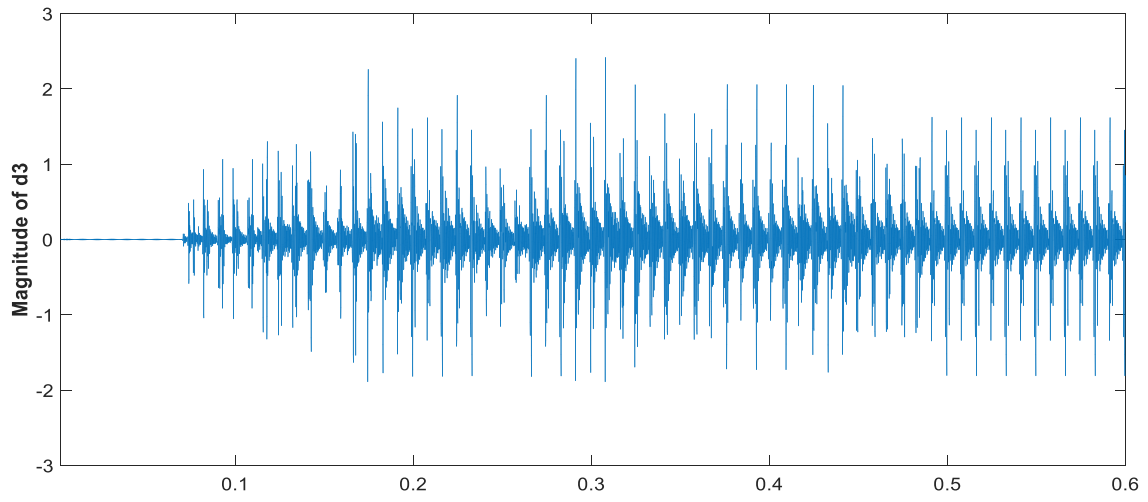| Method	dependability	Security	Train Accuracy	Test Accuracy
IEEE 13-Bus				
SVM	96.97	96.87	98.23	96.97
PNN	98.48	71.87	90.66	89.80
Feature	$F_{23} - F_{17} - F_8 - F_6 - F_2$			
IEEE 34-Bus				
SVM	94.29	100	98.28	96.55
PNN	91.43	97.83	96.35	94
Feature	$F_{45} - F_{32} - F_{28} - F_7 - F_4 - F_2$			
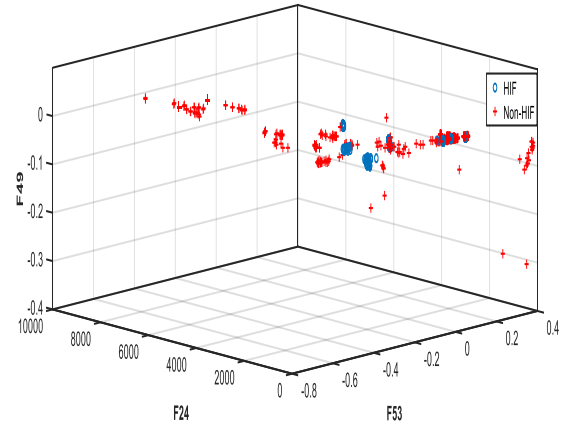
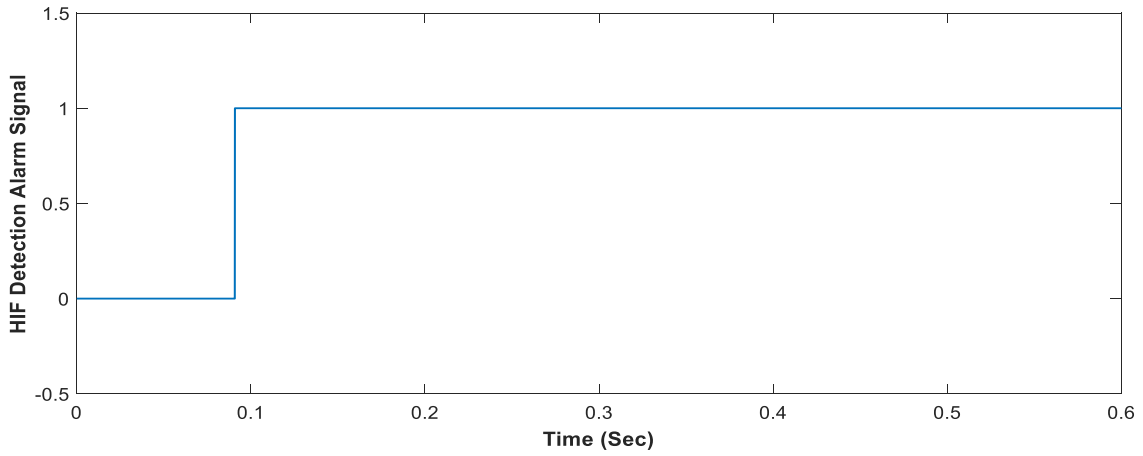a)   IEEE 13-Bus system
b)   IEEE 34-Bus system
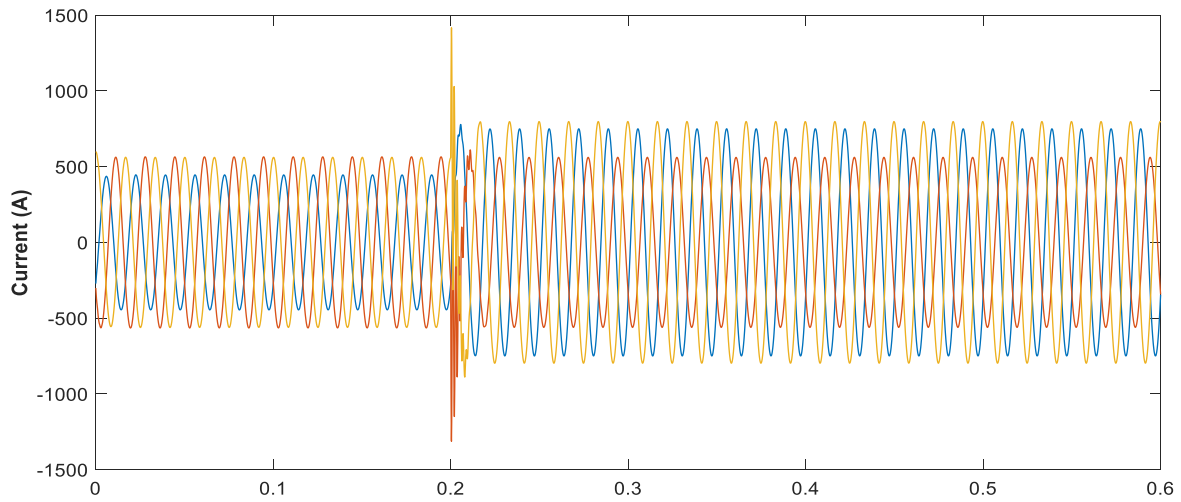Fig. 8. Best 3D representation of HIF and Non-HIF Feature in a) IEEE 13-bus b) IEEE 34-bus
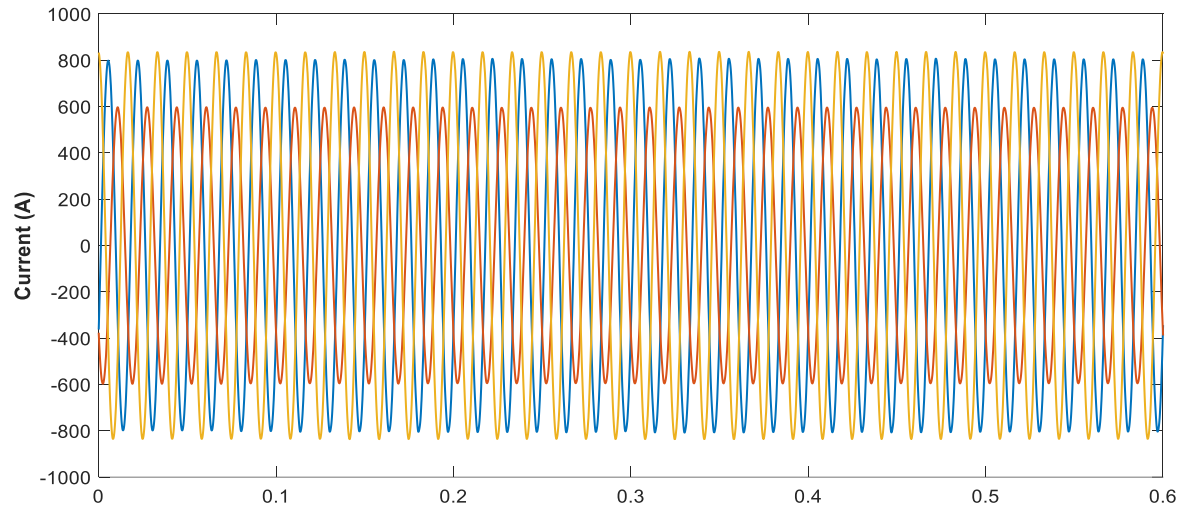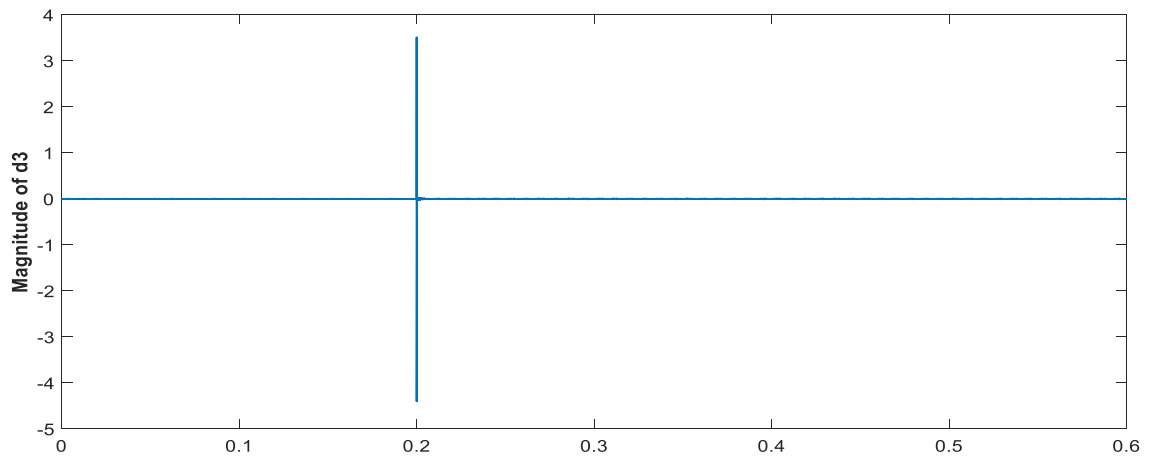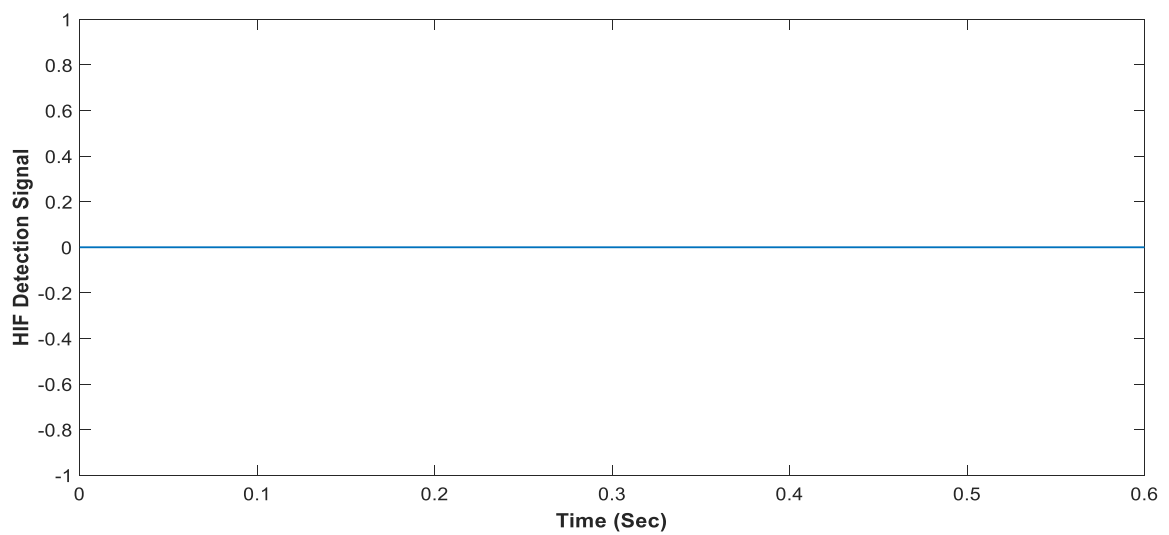
(a)

(b)

(c)

Fig. 9. Performance of the algorithm for HIF fault (a) Three phase current waveform (b) magnitude of detail coefficients at level 3, and (c) Detection signal

Fig. 10. Performance of algorithm for load switching event (a) Three phase current waveform (b) magnitude of detail coefficients at level 3, and c) Detection signal

As shown in In Fig 9(c), the HIF detection signal in HIF condition is activated two cycles after the fault inception. However as shown in Fig. 10(c), the HIF detection signal under the load switching event is not activated. According to the simulation results obtained for IEEE 13-Bus and IEEE 34-Bus, a remarkable improvement in HIF detection accuracy is obtained by utilizing the correlation coefficients index beside the other extracted statistical indices. As reported in Table 3, the highest accuracy is achieved by GA-SVM method for both test systems. The highest accuracy is 98.99 % and 98.27 % for IEEE 13-Bus and IEEE 34-Bus test systems.

In [20], the accuracies of the SVM algorithm, Bayse, Parzen and Nearest Neighbor (NN) algorithms have been reported. As given in [20], the best accuracy for Bayes, NN, Parzen, SVM-Linear, SVM-Polynominal, SVM_RBF, has been obtained as 80 %, 97.5%, 92.5%, 77.5%, 97.5%, and 97.5% respectively. However, according to Table 4, the accuracy of the proposed method of this paper, is equal to 98.27% and 98.299% for IEEE 13-Bus and IEEE 34-Bus test systems, respectively.

4. Conclusion

In this paper, a reliable HIF detection method based on pattern recognition is proposed. To extract features in time-frequency domain the discrete wavelet transform is used. This process is performed by decomposing two cycles of fault current signal and extracting statistical features from detail coefficients of DWT in each level. After fault signal decomposition, correlation coefficients are introduced a new index. Only some features from 56 features are chosen by decision tree and GA as input features for classification methods. The results of dimension reduction proved that correlation coefficients have high information gain and priority. Also, the results of simulation in IEEE standard test systems have illustrated that the proposed method is more accurate in comparison with other implemented methods.

References

[1] A. V. Masa, S. Werben and J. C. Maun, "Incorporation of data-mining in protection technology for high impedance fault detection," *2012 IEEE Power and Energy Society General Meeting*, San Diego, CA, 2012, pp. 1-8.

[2] Carr, J. "Detection of high impedance faults on multi-grounded primary distribution systems." *IEEE Transactions on Power Apparatus and Systems* 4.PAS-100 (1981): 2008-2016.

[3] Lee, Robert E., and M. T. Bishop. "Performance testing of the ratio ground relay on a four-wire distribution feeder." *IEEE transactions on power apparatus and systems* 9 (1983): 2943-2949.

[4] Sultan, A. F., G. W. Swift, and D. J. Fedirchuk. "Detecting arcing downed-wires using fault current flicker and half-cycle asymmetry." *IEEE Transactions on Power Delivery* 9.1 (1994): 461-470.

[5] Mamishev, A. V., B. Don Russell, and Carl L. Benner. "Analysis of high impedance faults using fractal techniques." *Power Industry Computer Application Conference, 1995. Conference Proceedings., 1995 IEEE*. IEEE, 1995.

[6] Lee, I. *High-impedance fault detection using third-harmonic current. Final report*. No. EPRI-EL-2430. Hughes Aircraft Co., Malibu, CA (USA), 1982.

[7] Lien, Keng-Yu. "Energy variance criterion and threshold tuning scheme for high impedance fault detection." *IEEE Transactions on Power Delivery* 14.3 (1999): 810-817.

[8] Russell, B. Don. "Detection of arcing faults on distribution feeders." *Final Report Texas A&M Univ., College Station. Research Foundation.* 1 (1982).

[9] Huang, Shyh-Jier, and Cheng-Tao Hsieh. "High-impedance fault detection utilizing a Morlet wavelet transform approach." *IEEE Transactions on Power Delivery* 14.4 (1999): 1401-1410.

[10] Lai, T. M.. "High-impedance fault detection using discrete wavelet transform and frequency range and RMS conversion." *IEEE Transactions on Power Delivery* 20.1 (2005): 397-407.

[11] Michalik, Marek. "High-impedance fault detection in distribution networks with use of wavelet-based algorithm." *IEEE Transactions on Power Delivery* 21.4 (2006): 1793-1802.

[12] Elkalashy, Nagy I. "Modeling and experimental verification of high impedance arcing fault in medium voltage networks." *IEEE Transactions on Dielectrics and Electrical Insulation* 14.2 (2007): 375-383.

[13] Samantaray, S. R., B. K. Panigrahi, and P. K. Dash. "High impedance fault detection in power distribution networks using time-frequency transform and probabilistic neural network." *IET generation, transmission & distribution* 2.2 (2008): 261-270.

[14] Benner, Carl L., and B. Don Russell. "Practical high-impedance fault detection on distribution feeders." *IEEE Transactions on Industry Applications* 33.3 (1997): 635-640.

[15] Girgis, Adly A., Wenbin Chang, and Elham B. Makram. "Analysis of high-impedance fault generated signals using a Kalman filtering approach." *IEEE Transactions on Power delivery* 5.4 (1990): 1714-1724.

[16] Sheng, Yong, and Steven M. Rovnyak. "Decision tree-based methodology for high impedance fault detection." *IEEE Transactions on Power Delivery* 19.2 (2004): 533-536.

[17] Michalik, Marek. "New ANN-based algorithms for detecting HIFs in multigrounded MV networks." *IEEE transactions on power delivery* 23.1 (2008): 58-66.

[18] Eissa, M. M., GM A. Sowilam, and A. M. Sharaf. "A new protection detection technique for high impedance fault using neural network." *2006 Large Engineering Systems Conference on Power Engineering*. IEEE, 2006.

[19] M. Haghifam, A. Sedighi and O. Malik, "Development of a fuzzy inference system based on genetic algorithm for high-impedance fault detection", *IEE Proceedings -*

Generation, Transmission and Distribution, vol. 153, no. 3, p. 359, 2006.

[20] Sarlak, M., and S. M. Shahrtash. "High impedance fault detection in distribution networks using support vector machines based on wavelet transform." *Electric Power Conference, 2008. EPEC 2008. IEEE Canada*. IEEE, 2008

[21] Sarlak, Mostafa, and S. Mohammad Shahrtash. "High-impedance faulted branch identification using magnetic-field signature analysis." *IEEE Transactions on Power Delivery* 28.1 (2013): 67-74

[22] Ghaderi, Amin. "High-Impedance Fault Detection in the Distribution Network Using the Time-Frequency-Based Algorithm." *IEEE Transactions on Power Delivery* 30.3 (2015): 1260-1268.

[23] S. Chakraborty and S. Das, "Application of Smart Meters in High Impedance Fault Detection on Distribution Systems," in IEEE Transactions on Smart Grid. doi: 10.1109/TSG.2018.2828414

[24] M. Kavi, Y. Mishra and M. D. Vilathgamuwa, "High-impedance fault detection and classification in power system distribution networks using morphological fault detector algorithm," in *IET Generation, Transmission & Distribution*, vol. 12, no. 15, pp. 3699-3710, 28 8 2018.

[25] K. Sarwagya, S. De and P. K. Nayak, "High-impedance fault detection in electrical power distribution systems using moving sum approach," in *IET Science, Measurement & Technology*, vol. 12, no. 1, pp. 1-8, 1 2018.

[26] W. C. Santos, F. V. Lopes, N. S. D. Brito and B. A. Souza, "High-Impedance Fault Identification on Distribution Networks," in IEEE Transactions on Power Delivery, vol. 32, no. 1, pp. 23-32, Feb. 2017.

[27] Graps, Amara. "An introduction to wavelets." *IEEE computational science and engineering* 2.2 (1995): 50-61.

[28] Akay, Mehmet Fatih. "Support vector machines combined with feature selection for breast cancer diagnosis." *Expert systems with applications* 36.2 (2009): 3240-3247.

[29] Burges, Christopher JC. "A tutorial on support vector machines for pattern recognition." Data mining and knowledge discovery 2.2 (1998): 121-167

[30] Huang, Cheng-Lung, and Chieh-Jen Wang. "A GA-based feature selection and parameters optimization for support vector machines." Expert Systems with applications 31.2 (2006): 231-240.

[31] Feeders, Distribution Test. "Ieee pes distribution system analysis subcommittee." Online Available: http://www. ewh. ieee. org/soc/pes/dsaco m/testfeeders/index. html (2011).

[32] Emanuel, A. E. "High impedance fault arcing on sandy soil in 15 kV distribution feeders: contributions to the evaluation of the low frequency spectrum." *IEEE Transactions on Power Delivery* 5.2 (1990): 676-686.

[33] Grabczewski, Krzysztof. "Feature selection with decision tree criterion." (2005).

[34] Sugumaran, V., V. Muralidharan, and K. I. Ramachandran. "Feature selection using decision tree and classification through proximal support vector machine for fault diagnostics of roller bearing." *Mechanical systems and signal processing* 21.2 (2007): 930-942.